

# Effects of chemical weathering on infrared spectra of Columbia River Basalt and spectral interpretations of martian alteration

Joseph R. Michalski<sup>\*</sup>, Michael D. Kraft, Thomas G. Sharp, Philip R. Christensen

*Department of Geological Sciences, Arizona State University, Tempe, Arizona, 85287-1404, United States*

Received 23 February 2006; received in revised form 14 June 2006; accepted 20 June 2006

Available online 31 July 2006

## Abstract

We investigated the mineralogy of basalt weathering rinds and fresh basaltic rocks using visible/near-infrared (VNIR) ( $\lambda=0.4\text{--}2.5\ \mu\text{m}$ ) and thermal emission ( $\lambda=6\text{--}30\ \mu\text{m}$ ) spectroscopy to 1) constrain the effects of chemical weathering on rock spectra, and 2) further understand the context of infrared spectra of Mars, which may contain evidence for weathered rocks and particulates derived from them. VNIR spectra of weathered rock surfaces are generally redder and brighter than fresh surfaces. Thermal infrared spectra of weathered basalts show evidence for aluminous opal and clay minerals (or clay precursor mineraloids) in natural surfaces. Supporting VNIR observations generally do not show the same evidence for neoformed clays or silica because of their textural occurrence as thin coatings and microfracture-fill, and possibly due to poor crystallinity of the aluminosilicate weathering products in this context. Spectral trends observed at Mars, such as the detection of low to moderate (10–25%) abundances of silica and clay that are observed in the thermal infrared but not in the VNIR, are therefore consistent with trends observed for natural rock surfaces in the laboratory. The combined use of thermal infrared and VNIR suggest that vast areas of martian dark regions contain sandy–rocky basaltic materials with weathering rinds and thin coatings that could have formed in conditions of relatively low water/rock ratios.

© 2006 Elsevier B.V. All rights reserved.

*Keywords:* Mars; weathering; spectroscopy; Mineralogy; alteration

## 1. Introduction and background

Weathering rinds and rock coatings form on subaerially exposed or shallowly buried rocks as a function of their mineralogical and textural susceptibility to weathering, the availability of water, and the amount of time the rocks were exposed to particular environmental conditions [1]. On Mars, rocky and sandy surface materials may develop weathering rinds and coatings through time depending on their mineralogical and textural susceptibility, surface exposure age,

availability of water, or exposure to acid volatiles. Revealing the mineralogy and distribution of weathered rock surfaces on Mars is central to understanding the climate history of Mars, constraining styles of aqueous alteration, and establishing geologic surface ages.

Spectroscopic measurements of martian dark regions provide insight into weathering processes affecting sandy and rocky materials on Mars. Visible/near-infrared (VNIR) ( $\lambda=0.4\text{--}2.5\ \mu\text{m}$ ) reflectance spectra indicate that martian dark regions are largely composed of variably oxidized basaltic materials [2–4]. VNIR data show evidence for clay minerals in a limited number of sites representing ancient alteration of possible sedimentary or hydrothermal origin [5], but do not show evidence for

<sup>\*</sup> Corresponding author.

*E-mail address:* [michalskijoe@gmail.com](mailto:michalskijoe@gmail.com) (J.R. Michalski).

widespread, abundant clay minerals [2,4]. From these data, it seems that martian dark regions are composed of relatively unaltered basaltic materials, as they appear oxidized, but clay-poor. Thermal emission ( $\lambda=6\text{--}30\ \mu\text{m}$ ) spectra of Mars show evidence for widespread basaltic materials in dark regions as well [6–9]. However, thermal emission spectra also show evidence for low abundances ( $\sim 15\%$ ) of clay minerals (or poorly crystalline aluminosilicates similar to clays) throughout dark regions [10] and moderate abundances (5–25%) [9] of aluminous silica [11]. Originally these results were thought to represent purely igneous diversity of Mars [6–8], but the possibility that much of the spectral diversity is related to chemical weathering is an open question [10–16]. The northern lowlands of Mars, where high concentrations of silica and/or clays are observed in the thermal infrared, are devoid of VNIR spectral features related to igneous or alteration minerals [17]. However, these regions do exhibit a blue-slope in the VNIR which could indicate the presence of coatings and rinds on rocky materials [17].

Interpretations of infrared measurements for weathering on Mars are fraught with questions and complications. Infrared spectroscopic data provide mineralogical information about the uppermost 10s of  $\mu\text{m}$  of geologic materials and could well be sensitive to thin weathering rinds and coatings on martian rocks and sand. But, the differences between thermal infrared and VNIR observations of Mars are cause for concern. If thermal emission data show evidence for widespread silica and clays (or clay-like mineraloids) on Mars, why are they not observed in the VNIR? Given that spectra of Mars contain abundant evidence for primary minerals, can the surfaces be chemically weathered? In this paper, we present the results of a spectroscopic study of “weathered” and “fresh” basalts from the Columbia River Basalt Group (CRBG) employing both VNIR and thermal emission wavelengths. We demonstrate some of the spectral trends observed for weathered surfaces and consider the implications for interpreting martian surface alteration from infrared spectral data.

## 2. Methods

Thirty cobble-sized (6–10 cm-diameter) rock samples of basalt–icelandite were collected from the CRBG in central to southeastern Washington State. Samples were collected from all major formations of the CRBG, including (in decreasing age from approximately 17 to 6 Ma) the Innaha Formation, Grand Rhonde Basalt, Wanapum Basalt, and Saddle Mountains Basalt. For more information on the volcanology, petrology, and geochemistry of CRBG rocks sampled, see [18–20].

Absolute surface exposure ages are not known for the sample sites, but rocks were collected from a range of relative exposure ages from old ( $\leq 10\ \text{ka}$ ), rocky surfaces on top of topographic highs to young anthropomorphic exposures.

All rock samples were analyzed by bulk-powder X-ray diffraction (XRD), VNIR spectroscopy, and thermal emission spectroscopy. Select samples were analyzed by optical petrography and scanning electron microscopy (SEM). Detailed mineralogical analyses of selected samples have been reported by [21]. XRD analyses were performed from  $5$  to  $65^\circ\ 2\theta$  on bulk-powders and from  $2$  to  $70^\circ\ 2\theta$  on selected  $< 2\ \mu\text{m}$  size fractions. Bidirectional VNIR spectra of rock chips were collected (from  $\lambda=0.35$  to  $2.55\ \mu\text{m}$ ) at the Brown University RELAB facility. Rock chips were prepared by cutting or breaking open the interior of the rock into 1–2 cm-sized pieces, in the case of “fresh samples,” or breaking off 1–2 cm-sized pieces of the natural surface in the case of “weathered surfaces.” The field of view for each spectral measurement was an ellipse with a major axis of  $\sim 3\text{--}10\ \text{mm}$ , which is sufficient area to sample the bulk composition of these aphanitic to plagioclase-porphyrific rocks. Band depth measurements [22] were applied to rock spectra using the Eq. (1), where  $BD$  is the band depth,  $R_c$  is the reflectance of the continuum slope, and  $R_b$  is the reflectance of the band center.

$$BD = 1 - \frac{R_b}{R_c} \quad (1)$$

Thermal infrared emission spectra of fresh and weathered surfaces of the same samples were acquired at Arizona State University (from  $\lambda=5\text{--}50\ \mu\text{m}$ ) [23]. These spectra were quantitatively analyzed by a linear spectral deconvolution, which mathematically constrains mineral abundances by modeling a mixed scene (i.e. rock) spectrum [24–26]. Spectral deconvolution was performed over the  $7.7\text{--}28.6\ \mu\text{m}$  ( $350\text{--}1300\ \text{cm}^{-1}$ ) spectral range using input library end-members including a range of plagioclase and K-feldspar compositions, felsic and basaltic volcanic glasses, various pyroxenes, several Fe- and Fe–Ti-oxides, and various clay minerals. See [27] for more background information on spectral data processing.

## 3. Spectra of fresh basalt surfaces

VNIR spectra of fresh CRBG rock surfaces contain five major absorptions at ( $\lambda\cong$ ) a)  $0.7\text{--}1\ \mu\text{m}$ , b)  $1.05\ \mu\text{m}$ , c)  $1.41\ \mu\text{m}$ , d)  $1.91\ \mu\text{m}$ , and e)  $2.32\ \mu\text{m}$  (Fig. 1), corresponding to a)  $\text{Fe}^{3+}$  electronic absorptions in oxides/

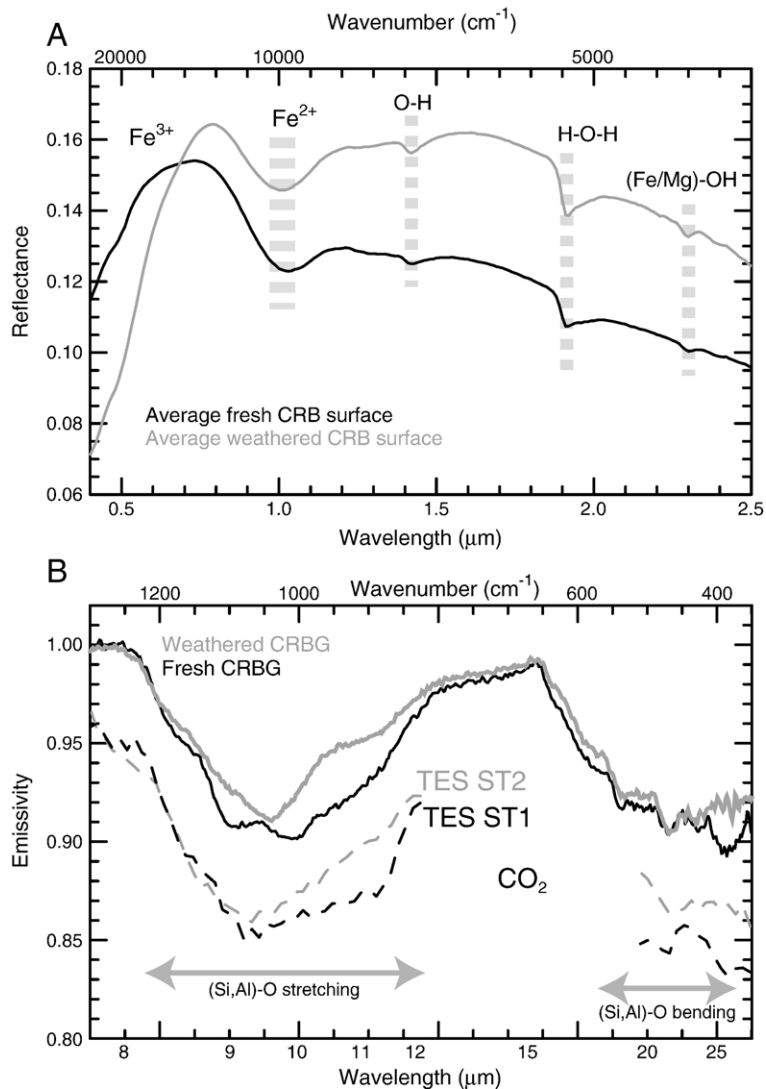


Fig. 1. Average VNIR (A) and thermal emission (B) spectra of fresh and weathered surfaces of CRBG samples. Major absorptions are shown. TES surface type spectra (Bandfield et al., 2000) are also shown (but are missing the spectral range where CO<sub>2</sub> absorbs at Mars).

hydroxides, b) Fe<sup>2+</sup> electronic absorptions in pyroxene, c) O–H vibrations in hydroxyl, d) H–O–H vibrations in mineralogic water, and e) M–OH vibrations in clay minerals (M=metals, Fe<sup>2+</sup> or Mg<sup>2+</sup> in this case). The Fe<sup>3+</sup> absorption at short wavelengths is generally weak in fresh surfaces. The placement of the pyroxene absorption near 1.05 μm indicates the presence of a high-calcium pyroxene (HCP) in all samples, consistent with detection of augite in all samples by XRD. The broad 2 μm pyroxene band observed in spectra of pure pyroxene samples is weak in these rocks, masked by the presence of hydration bands (c–e). The absorptions at 1.41 μm, 1.91 μm, and 2.32 μm can all be satisfactorily explained by the presence of a Mg-rich TOT clay mineral such as

saponite (by TOT, we mean sheet silicate containing layers composed of bonded tetrahedral, octahedral, and tetrahedral sheets, *i.e.* a 10.5 Å phyllosilicate). The three hydration absorptions are mutually correlated suggesting that a single phase (or multiple phases with similar mineralogical characteristics) is responsible for these absorptions in most rocks (Fig. 2). A broad XRD-peak located near  $d=13\text{--}14.5$  Å in many of the data is interpreted as evidence for expanded TOT (smectite?) or chlorite clay and a random amount of the <2 μm size fraction indicates the presence of trioctahedral clay, based on the observation of a {060} diffraction peak near  $d=1.535$  Å. Patchy brown replacements of interstitial glass observed petrographically are the likely context of

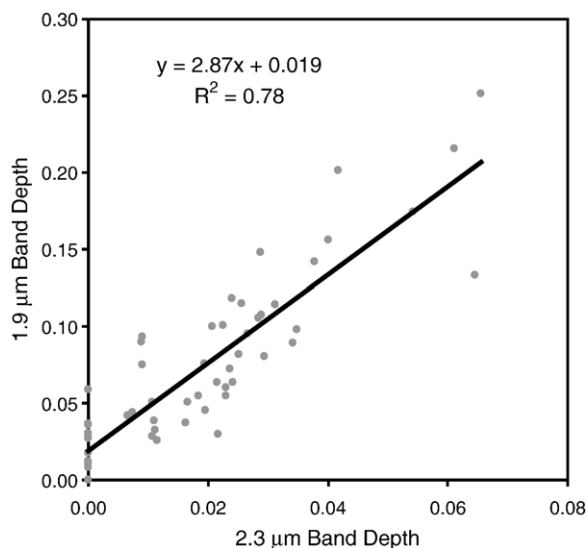


Fig. 2. The scatter plot shows that the 1.9  $\mu\text{m}$  H–O–H absorption strength is correlated with the M–OH absorption strength, suggesting that both absorptions are caused by a single phase or multiple phases with similar characteristics.

the Mg-rich clay mineral(s) detected spectroscopically and with XRD. Mg- and Fe-bearing clay minerals observed in the same context in CRBG rocks by [20] were interpreted as a low-temperature, hydrothermal phenomenon, and we agree with this interpretation.

Thermal emission spectra of fresh surfaces contain strong, overlapping absorptions at ( $\lambda \approx$ ) a) 8–12  $\mu\text{m}$ , b) 20–25  $\mu\text{m}$ , c) 15–20  $\mu\text{m}$ , and d) 25–30  $\mu\text{m}$  (Fig. 1) related to a) (Si, Al)–O stretching vibrations, b) (Si, Al)–O bending vibrations, and c)  $\text{M}^{\text{IV}}$ –O vibrations, and d)  $\text{M}^{\text{VI}}$ –O vibrations. Linear spectral deconvolution of fresh surface spectra suggests average compositions of 58% plagioclase feldspar (generally andesine), 15% CPX (usually augite), 10% basaltic glass (50%  $\text{SiO}_2$ ), 5% felsic glass (78%  $\text{SiO}_2$ ), 5% clay minerals (saponite, serpentine, and nontronite), and trace abundances of olivine, Fe-oxides, and alkali feldspars. These results are consistent with the detection of andesine and augite by XRD in all rocks.

#### 4. Spectra of weathered basalt surfaces

VNIR spectra of natural, weathered surfaces exhibit the same five absorptions as the fresh rock spectra, but there are some important differences. Overall, the weathered surfaces are brighter ( $\sim 16\%$  greater reflectance) than the fresh surfaces. The  $\text{Fe}^{3+}$  absorption is much stronger for natural surfaces, giving them a brown-red color. The average band depths of the 1  $\mu\text{m}$  pyroxene absorption in weathered surfaces is  $\sim 23\%$

weaker than for fresh surfaces ( $\text{BD}=0.125$  for average fresh surfaces compared to 0.097 for average weathered surfaces). Hydration bands at 1.41  $\mu\text{m}$ , 1.91  $\mu\text{m}$ , and 2.32  $\mu\text{m}$  have slightly higher band depths for weathered surfaces than fresh on average, suggesting either increased hydration due to the weathering process, or higher relative stability of the bulk-rock Mg-clay minerals compared to igneous phases in the weathered surfaces. Al–OH absorptions located near ( $\lambda \approx$ ) 2.2  $\mu\text{m}$  in spectra of aluminous clays are not observed in weathered CRBG spectra, except for an extremely weak, broad absorption in one sample.

Thermal emission spectra of weathered surfaces are generally similar to spectra of fresh surfaces, but there are some key differences. Weathered surfaces have slightly less overall spectral contrast and less absorption near ( $\lambda \approx$ ) 11–12  $\mu\text{m}$ , in the position where absorptions related to depolymerized silicates such as pyroxene occur. The spectral minimum of average weathered surface spectra is located near ( $\lambda \approx$ ) 9.6  $\mu\text{m}$  compared to 10  $\mu\text{m}$  in fresh rock surfaces, indicating an overall higher silica content of the weathered surfaces. Linear deconvolution of weathered surface spectra indicates average surface compositions of 30% plagioclase feldspar, 8% alkali feldspar (albite and orthoclase), 11% CPX (dominantly augite), 5% basaltic glass, 5% felsic glass (or aluminous, amorphous silica), 5% opal-A, 26% clay minerals, and 9% Fe-oxides. Modeled clay minerals include Mg-bearing trioctahedral clays (saponite, serpentine), Fe-bearing dioctahedral clays (nontronite), and abundant Al-bearing dioctahedral clays (illite and montmorillonite). Spectral model results for each weathered sample generally include high abundances ( $\sim 20$ –40%) of only one of the following: 1) aluminous clay minerals, 2) K-feldspar, or 3) felsic volcanic glass/aluminous silica, suggesting that these three materials are somewhat interchangeable in the modeling process. K-feldspar is only a trace mineral in these rocks, primary felsic glass is not enriched in rock surfaces, and supporting evidence for crystalline clay minerals (within rock surfaces) is tenuous at best; the reason for these incorrect model results is an open question. Do they correspond to actual aluminosilicate alteration products that are not currently represented by spectral library minerals? Do they result entirely from geometric effects producing non-linear mixing of spectra of natural surfaces? Or, is it a combination of these effects?

#### 5. Discussion

There are several important differences between the spectral properties of basalt weathering rinds in the VNIR

versus the thermal infrared. Thermal emission spectra of many of the weathered surfaces are similar to spectra of clay minerals, and aluminous clay minerals in particular (Fig. 3). However, the VNIR spectra of these same surfaces do not show evidence for aluminous clay minerals. Similarly, many of the thermal emission spectra of weathered surfaces contain strong absorptions indicative of (aluminous) opaline silica, while the VNIR spectra of these same surfaces do not show evidence for opal (Fig. 3).

The spectral disconnect between the two techniques can be understood in terms of the differences in type and strength of absorptions observable in the two wavelength ranges. Thermal emission spectra of clay minerals are dominated by (Si, Al)–O stretching and bending absorp-

tions related to the tetrahedral sheets of the clays. These absorptions are strong (have high absorption coefficients) and therefore the thermal infrared technique is sensitive to even small abundances or thin coatings of clay minerals or clay-like materials. In the VNIR, clay absorptions correspond to O–H and M–OH bonds in the octahedral sheets, and to H–O–H bonds in interlayer sites. In general, these bands are weaker than the thermal infrared absorptions, in particular if the physical nature of the materials is such that multiple reflections are limited (as is the case in rocky materials). This is further complicated by the issue of crystallinity; spectral absorptions become more spread out and therefore weaker at a specific wavelength with decreasing crystal ordering. The spectral

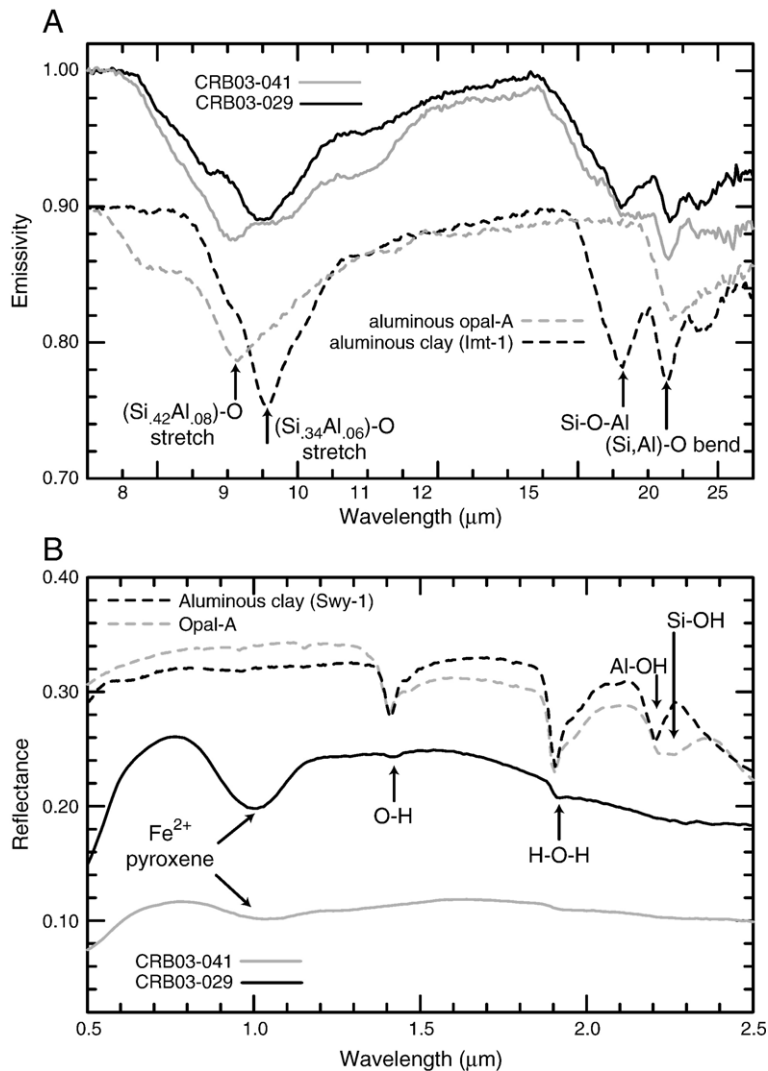


Fig. 3. Examples of the spectral differences observed between VNIR and thermal emission measurements. Thermal emission spectra of many weathered surfaces show evidence for aluminous clay-rich or silica-rich surfaces (A), but VNIR of these same surfaces do not show evidence for opaline silica or aluminous clays.

disconnect with regard to CRBG rock surfaces can therefore be explained if the thermal emission spectra are detecting small abundances of clay minerals or poorly crystalline aluminosilicates that are compositionally similar to clay minerals, but the abundances, crystallinity, and geometry of such materials in the rock surfaces renders them undetectable to VNIR. Similar to clay minerals, opaline silica is a strong absorber in the thermal infrared. In the VNIR, opal is only detectable by its weaker Si-OH absorptions located near ( $\lambda=$ ) 2.23  $\mu\text{m}$ . Thin coatings of silica and clay-like materials on rocky surfaces may be much less detectable with VNIR spectroscopy compared to thermal infrared spectroscopy. Even thin silica coatings (<5  $\mu\text{m}$ -thick) have a strong impact on emission spectral measurements [13].

Petrographic observations provide context for the spectroscopic interpretations discussed above. Optical and SEM observations show that the weathering rinds of these rocks are composed mostly of primary igneous phases, but contain microcracks filled with aluminosilicate material. The aluminosilicate fracture fill and coatings are compositionally similar to clay minerals and aluminous silica (Fig. 4). Silica-rich coatings are observed on the exterior of some rocks, and in some cases it is philosophically difficult to distinguish between penetrative rock coatings forming in near-surface fractures and in-situ weathering of primary phases in fractures. The aluminosilicate weathering products found in near-surface voids are compositionally distinct from Mg-rich, hydrothermal alteration products found throughout the samples. We attribute the thermal emission spectral signature of glass, silica, and clay minerals in weathered

surfaces to these near-surface aluminosilicate materials that occur as fracture fill, rock coatings, and/or penetrative coatings [21].

The spectral features of basalt weathering rinds provide insights into weathering processes affecting rock surfaces. In both the VNIR and thermal infrared, the spectral character of weathering rinds is usually dominated by primary phases. Spectral evidence for neoformed crystalline clay minerals within weathering rinds is lacking, though there is abundant evidence for poorly crystalline aluminosilicates. The well-crystalline clays that are detected in our rocks are related to ancient hydrothermal activity and these clays, similar to pyroxene and plagioclase, are weathering out of rock surfaces. Our results are consistent with other studies of weathering rinds on volcanic rocks. Colman [28–29] points out that aluminosilicate materials, which are compositionally clay-like but x-ray amorphous, are much more common than crystalline phyllosilicates in weathering rinds. Formation of x-ray amorphous aluminosilicate is regarded by some as the usual initial phase of rock weathering, where the degradation of rocks ultimately leads to formation of crystalline clay minerals in soil environments [30]. In addition, amorphous silica (relatively pure or aluminous opal-A) is a common constituents of rock coatings (in addition to weathering rinds) in arid climates [1].

## 6. Conclusions

These results have important implications for interpreting chemical weathering processes on Mars from

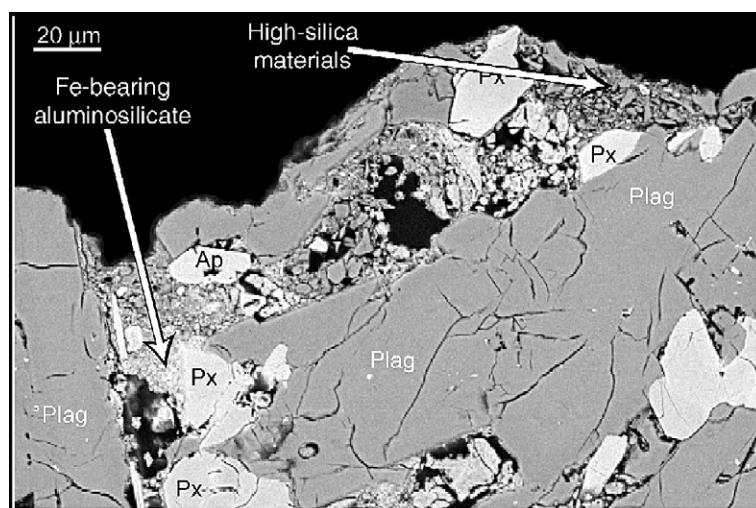


Fig. 4. Backscattered electron image of a basalt weathering rind (sample CRB04049). Mineral phases include plagioclase (Plag), clinopyroxene (Px), and apatite (Ap). Cracks are filled with aluminosilicate materials. More aluminous materials also have higher Fe-content, possibly related to finely disseminated Fe-oxides/hydroxides.

spectral data. Based on these results, which are admittedly of limited scope, the spectral trends expected for natural, weathered basalt surfaces are: 1) reddening and brightening of rocks in the VNIR region, 2) increase in apparent silica content from thermal infrared spectra, and 3) increase in clay content from thermal infrared measurements. Martian surfaces show these same trends—variably oxidized surfaces and the presence of amorphous silica and clay-like materials in the thermal infrared. Although VNIR instrumentation does not see enhanced features related to silica or crystalline clays in the vast areas where thermal infrared instruments see clays and silica, this is not a contradiction if the materials occur in weathered rock surfaces as fracture fill and thin coatings; a plausible context for alteration materials on Mars. Sandy–rocky surfaces made up of impact ejecta, dunes, flood sediments, and eroded lavas may have been exposed to acid volatiles in the atmosphere or surface water (related to frosts, snowmelt, or other transient events) over vast periods of time. It is possible that small volumes of poorly crystalline alteration products are present within surface materials, related to relatively recent chemical weathering in conditions of low water/rock ratios. Further analyses of these spectral trends on Mars, especially at higher spatial resolution, will likely lead to breakthroughs in establishing surface exposure ages and understanding past occurrences of near-surface water.

## Acknowledgements

Funding for this work was provided by the Mars Fundamental Research Program grant #NNG05G149G (to TGS) and by the Planetary Imaging and Analysis Facility and Advanced Training Institute grant #1230449 (PRC). We thank Douglas Ming, Richard Morris, Stephen Reidel, Peter Hooper, Takahiro Hiroi, Victoria Hamilton, Michael Wyatt, Archana Nair, and John Mustard for insightful conversations and logistical support.

## References

- [1] Dorn, R. *Rock Coatings*, Elsevier, New York, 1998.
- [2] L.A. Soderblom, The composition and mineralogy of the martian surface from spectroscopic observations: 0.3  $\mu\text{m}$  to 50  $\mu\text{m}$ , in: H. H. Kieffer, B.M. Jakosky, C.W. Snyder, M.S. Matthews (Eds.), *Mars*, University of Arizona Press, Tucson, 1992, pp. 557–593.
- [3] J.F. Bell, et al., Mars surface mineralogy from Hubble Space Telescope imaging during 1994–1995: observations, calibration, and initial results, *J. Geophys. Res.* 102 (E4) (1997) 9109–9123.
- [4] J.P. Bibring, et al., Mars surface diversity as revealed by the OMEGA/Mars Express observations, *Science* (2005), doi:10.1126/science.1108806.
- [5] F. Poulet, J.-P. Bibring, J.F. Mustard, A. Gendrin, N. Mangold, Y. Langevin, R.E. Arvidson, B. Gondet, C. Gomez, Phyllosilicates on Mars and implications for early martian climate, *Nature* 438 (2005) 623–627, doi:10.1038/nature04274.
- [6] J.L. Bandfield, V.E. Hamilton, P.R. Christensen, A global view of martian volcanic compositions, *Science* 287 (2000) 1626–1630.
- [7] V.E. Hamilton, M.B. Wyatt, H.Y. McSween Jr., P.R. Christensen, Analysis of terrestrial and martian volcanic compositions using thermal emission spectroscopy 2. Application to martian surface spectra from the Mars Global Surveyor Thermal Emission Spectrometer, *J. Geophys. Res.* 106 (7) (2001) 14,733–14,746.
- [8] P.R. Christensen, et al., Mars Global Surveyor Thermal Emission Spectrometer experiment: investigation description and surface science results, *J. Geophys. Res.* 106 (E10) (2002) 23,823–23,871.
- [9] J.L. Bandfield, Global mineral distributions on Mars, *J. Geophys. Res.* 107 (E6) (2002) Art. No. 5042.
- [10] J.R. Michalski, M.D. Kraft, T.G. Sharp, L.B. Williams, P.R. Christensen, Emission spectroscopy of clay minerals and evidence for poorly crystalline aluminosilicates on Mars from Thermal Emission Spectrometer data, *J. Geophys. Res.* 111 (2006), doi:10.1029/2005JE002438.
- [11] J.R. Michalski, M.D. Kraft, T.G. Sharp, L.B. Williams, P.R. Christensen, Mineralogical constraints on the high-silica martian surface component observed by TES, *Icarus* 174 (2005) 161–177.
- [12] M.B. Wyatt, H.Y. McSween Jr., Spectral evidence for weathered basalt as an alternative to andesite in the northern lowlands of Mars, *Nature* 417 (2002) 263–266.
- [13] M.D. Kraft, J.R. Michalski, T.G. Sharp, Effects of pure silica coatings on thermal emission spectra of basaltic rocks: considerations for martian surface mineralogy, *GRL* 30 (24) (2003) 2288, doi:10.1029/2003GL018848.
- [14] R.V. Morris, T.G. Graff, S.A. Mertzman, M.D. Lane, P.R. Christensen, Palagonitic (not andesitic) Mars: evidence from thermal emission and VNIR spectra of palagonitic alteration rinds on basaltic rock, *Sixth Int. Conf. Mars, Pasadena, CA., 2003*, abstract #3211.
- [15] S.W. Ruff, Basaltic andesite or weathered basalt: a new assessment, *Sixth Int. Conf. Mars, Pasadena, CA., 2003*, abstract #3258.
- [16] M.B. Wyatt, H.Y. McSween Jr., K.L. Tanaka, J.W. Head III, Global geologic context for rock types and surface alteration on Mars, *Geology* 32 (8) (2004) 644–648.
- [17] J.F. Mustard, F. Poulet, A. Gendrin, J.-P. Bibring, Y. Langevin, B. Gondet, N. Mangold, G. Bellucci, Olivine and pyroxene diversity in the crust of Mars, *Science* 307 (2005) 1594–1597.
- [18] A.C. Waters, Stratigraphic and lithologic variations in the Columbia River Basalt, *Am. J. Sci.* 259 (8) (1961) 583–611.
- [19] Volcanism and tectonism in the Columbia River flood basalt province, in: S.P. Reidel, P.R. Hooper (Eds.), *GSA Special Pub.*, 1989, p. 239.
- [20] G. Caprarelli, S.P. Reidel, Physical evolution of the Grand Rhonde Basalt magmas, Columbia River Basalt Group, northwestern USA, *Miner. Petrol.* 80 (2004) 1–25.
- [21] M.D. Kraft, J.R. Michalski, T.G. Sharp, Thermal emission spectral modeling of weathered basalt surfaces, *LPSC XXXVII*, 2006 abstract #2449.
- [22] J.F. Mustard, C.D. Cooper, Joint analysis of ISM and TES spectra: the utility of multiple wavelength regimes for martian surface studies, *J. Geophys. Res.* 110 (E5) (2005) Art. No. E05012.
- [23] S.W. Ruff, P.R. Christensen, P.W. Barbera, D.L. Anderson, Quantitative thermal emission spectroscopy of minerals: a technique for measurement and calibration, *J. Geophys. Res.* 102 (1997) 14,899–14,913.
- [24] V.E. Hamilton, P.R. Christensen, H.Y.J. McSween, Determination of martian meteorite lithologies and mineralogies using vibrational spectroscopy, *J. Geophys. Res.* 102 (1997) 25,593–25,603.

- [25] M.S. Ramsey, P.R. Christensen, Mineral abundance determination: quantitative deconvolution of thermal emission spectra, *J. Geophys. Res.* 103 (1998) 577–596.
- [26] K.C. Feely, P.R. Christensen, Quantitative compositional analysis using thermal emission spectroscopy: application to igneous and metamorphic rocks, *J. Geophys. Res.* 104 (E10) (1999) 24,195–24,210.
- [27] Michalski, J.R., Silicate alteration mineralogy of the martian surface from TES: constraints from emission spectroscopy of terrestrial materials, Ph.D. Diss., Ariz. St. Univ., Tempe, Arizona, 2005.
- [28] S.M. Colman, Chemical weathering of basalts and andesites: evidence from weathering rinds, USGS Prof. Pap. (1981) 1246.
- [29] S.M. Colman, Clay mineralogy of weathering rinds and possible implications concerning the sources of clay minerals in soils, *Geology* 10 (1982) 370–375.
- [30] M.B. McBride, Environmental chemistry of soils, Oxford University Press, New York, 1994, 406 pp.